Circular array of anisotropic fibers: A discrete analog of a q plate

C. N. Alexeyev*

Taurida National V.I. Vernadsky University, Vernadsky Prospekt, 4, Simferopol, Crimea 95007, Ukraine

(Received 1 October 2012; published 26 December 2012)

In this paper, we have studied the propagation of light in a p array, that is, a circular array of strongly anisotropic fibers, orientation of whose anisotropy axes linearly depends on the angular position of the fiber in the array and makes an integer number of full rotations p while tracing along its contour. We have obtained the spectrum and the structure of supermodes for such a system and have shown that they consist of two discrete optical vortices nestled in the opposite circular polarizations. We have found the expressions for topological charges of such vortices. We have also studied the angular momentum carried by these supermodes. We have obtained the expression for the evolution of an arbitrary excitation created at the array's input upon its discrete diffraction in the array. As an example, we have examined the propagation of the set of circularly polarized fundamental modes excited at the input end with equal weights and phases. We have demonstrated that, in certain cross sections, the p array generates a discrete circularly polarized optical vortex, whose topological charge is determined by the array's index p. In this way, we have shown that the p arrays enable polarization control over phase singularities being a discrete analog of the q plates.

DOI: 10.1103/PhysRevA.86.063830 PACS number(s): 42.81.Qb, 42.25.Bs, 42.50.Tx

I. INTRODUCTION

Since early pioneering writings on dislocations of wave fronts and phase singularities [1], it has been reliably established that, save for few particular cases, vectorial fields do not allow the existence of singularity points where the field vanishes. This is explained through the impossibility to make, in a general case, three complex scalar functions, which describe three components of a vectorial field, simultaneously equal to zero. On the contrary, for a scalar field Ψ, this task is easily fulfilled, and the location of such zero intensity points (actually forming spatial lines, threads of darkness) is determined by the equationRe $\Psi = \text{Im}\ \Psi = 0$. Such points are also known to nestle optical vortices (OVs) [2]. Although studying OVs remains one of the key problems of singular optics [3], at present, it is concerned with a much broader scope of problems, which, to mention a few, include caustic singularities [4], polarization singularities or singularities of vectorial fields [5], correlation singularities [6], and others [7]. These researches showed that, in general, singularities of the scalar field type do not exist in the vectorial case, this fact being an example of the concept of hierarchy of singularities, according to which the higher-order singularities cancel the lower-order ones [8]. In this way, in a sense, vectorial properties of the electromagnetic field are kind of antagonistic to its scalar ones.

Luckily, this is only one of the aspects of their involved interconnection. Making the question of the existence of zero-intensity points more problematic, the vectorial nature of the electromagnetic field opens great possibilities in controlling the properties of phase singularities in the field's components. A natural mechanism, enabling such polarization control over phase singularities, is embedded into any vectorial field and is associated with the spin-orbit interaction (SOI). First introduced in optics by Liberman and Zel'dovich with the example of light's propagation in an optical fiber, until quite recently, this phenomenon has been mainly studied in the frameworks of fiber optics providing impressive examples of such related effects as the optical Magnus effect and others [9]. Modern papers have unveiled the presence of this phenomenon in other optical systems, including crystals and spatial-inhomogeneous systems [10], liquid crystals [11], as well as in a free space [12]. The SOI has been proven to play an essential part in the photonic spin Hall effect [13]. This interaction also underlies conversion of spin to orbital angular momentum (OAM) in metamaterials and at acousto-optic diffraction of light [14]. However, the most spectacular demonstration of its presence was achieved by using the so-called q plates in which the specially engineered distribution of local anisotropy axes in a planar system renders it the ability to convert regular beams into singular ones [15]. Basically, this technique involves manipulation with the beam's polarization so as to introduce a space-variant Pancharatnam-Berry phase as has been suggested by Bhandari [16] and first experimentally realized by Biener *et al.* [17] (for details, see also Ref. [18]). Analogous results are obtained through discrete manipulation with polarization states [19]. One should emphasize, though, that such engineering results in discrete phase fronts, which, in the case of the generation of OVs by such a technique, leads to decreasing in the OAM per photon connected with the deviation of the phase distribution from that characteristic to a pure OV.

The fact that even discrete geometries of q plates allow the generation of helical-front beams suggests studying the possibility of the creation of OVs in other polarization-variant discrete optical systems. In this paper, as such a system, we investigate circularly arranged arrays of anisotropic evanescently coupled fibers. The circular fiber array, being a well-known and a classical fiber optical system, is still being studied in connection with further elaboration of the model and with regard to novel applications [20]. In particular, circularly arranged fiber arrays draw the attention of research due to unique possibilities in the creation of OAM-carrying beams [21]. Concerning the model itself, it has been shown that the

*Corresponding author: c.alexeyev@yandex.ua

supermodes of circular arrays of ideal fibers represent the so-called discrete OVs (DVs) [22], which possess nonzero OAM. It proved even possible to introduce a certain lattice angular momentum (AM), connected with the additional conservation law in circular arrays of coupled fibers [23]. Although the possibility to control the OAM of supermodes by changing the geometrical parameters of the array was established, the range of OAM variations proved to be insufficient for practical applications. It is desirable to investigate the possibilities of a more effective OAM control in other types of circular arrays.

The aim of this paper is to study the propagation of light in a circular array of coupled strongly anisotropic fibers, whose anisotropy axes' orientation depends on the position of the fiber. We obtain the mode structure of such a system and show that, if the anisotropy axes make an integer number of full rotations p while tracing along the contour of the array, the supermodes consist of two DVs with opposite circular polarizations, whose topological charges are determined by the number p. We demonstrate that, in this way, circular arrays of anisotropic fibers enable polarization control over phase singularities. We also show that such a p *array* is able to transform an incident circularly polarized regular beam into a circular OV, being a discrete analog of the standard q plates in this way.

II. SUPERMODES OF ANISOTROPIC FIBER ARRAYS

As a model, consider a circular array of N evanescently coupled monomode weakly guiding optical fibers (cores, as a matter of fact) immersed into a medium with a universal refractive index n_{cl}. The centers of the cores are positioned at the vertices of a regular N-gon (see Fig. 1), and the cores are assumed to possess one-axis material anisotropy characterized by refractive indices n_e and n_o so that $n_e \approx n_o \approx n_{co}$, where n_{co} is the refractive index in the cores (steplike behavior is assumed). We also take that the refractive index contrast $\Delta = n_{co} - n_{cl} \ll 1$ satisfies $\Delta \gg n_e - n_o \equiv \Delta n$. One of the local principal axes of the refractive index tensor is perpendicular to the plane of the transverse cross section so that the transverse part of the refractive index tensor (written in the local frame) is $\hat{n}_t^2 = \mathrm{diag}(n_e^2, n_o^2)$. The other two regularly change their orientation in this plane as the number of the fiber $j = 0,1,\ldots,N-1$ increases

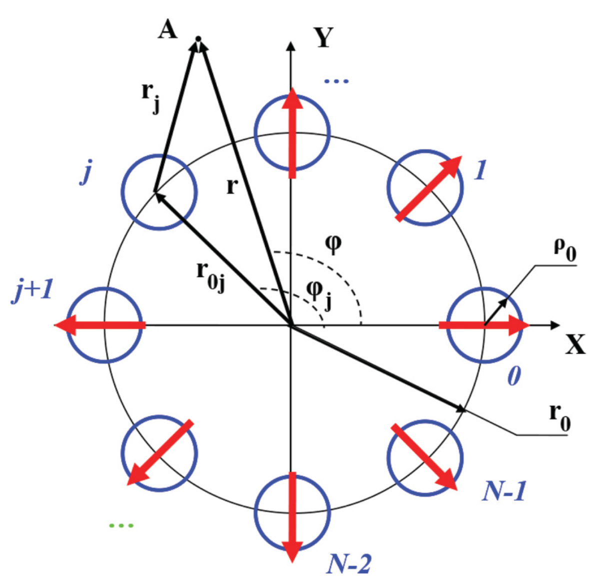

FIG. 1. (Color online) Geometry of a double-ring fiber array and the scheme of fibers' numeration. Red arrows indicate the anisotropy director's orientation. In the given example, the director vector makes one full rotation, which corresponds to the array's index $p = 1$.

$$\gamma_j^p = \frac{2\pi p}{N} j \equiv \varphi_p j, \tag{1}$$

where $p = 1,2,3,\ldots$ is the number of full rotations the anisotropy director makes while tracing the contour.

The question of propagation of light in two coupled anisotropic fibers has first been addressed by Shafir *et al.* [24] where it has been considered a general case of nonparaxial propagation in strongly coupled fibers at arbitrary orientation of anisotropy axes. Recently, this problem was revisited in connection with the spin angular momentum evolution in such a system [25]. By these studies, it has been established that, in a general case, the evolution of the state is rather complicated. However, the situation strongly simplifies in the case where the effect of anisotropy is much greater than the influence of evanescent coupling. Mathematically, this condition can be expressed as $\delta \equiv k^2 n_{co} \Delta n \gg a$, where δ characterizes anisotropy, a is the standard overlap integral (see, for example, Ref. [26]), and k is the wave number in vacuum. As can be shown, in strongly anisotropic coupled fibers, the coupling takes place only between the fields, which are similarly polarized in the local frames connected with the anisotropy axes. In this way, the evolution of the state factorizes in eigenpolarizations. This can also be explained in the following manner. As is known from the theory of coupled fibers, the most effective coupling is achieved if the fibers are identical or the propagation constants of the corresponding modes coincide. Otherwise, the energy transfer between the fibers is ineffective. Each fiber in the array of anisotropic fibers supports propagation of two orthogonally polarized modes, which are strongly split in propagation constants. Naturally, one can expect that the strongest coupling would occur for the modes with coinciding phase velocities, that is, the modes which possess similar polarization in the local frames, such as x'- or y'-polarized modes. Analysis of two coupled strongly anisotropic fibers shows that, in this case, normal modes of the system consist of symmetric and antisymmetric combinations of individual fiber modes with the same local polarization, say, $|x'L\rangle \pm |x'R\rangle$ where the first index specifies the type of linear polarization and the second—localization of the field on the left (right) fiber [24,25]. Such normal modes are analogous to normal modes of coupled identical mathematical pendulums. The "plus" sign in such interpretation corresponds to in-phase oscillations of the pendulums, whereas, the "minus" sign describes antiphase oscillations. This specific structure of normal modes is also inherent in ideal coupled fibers with the only difference that each individual fiber mode, in addition to a positioning index, also acquires the polarization marker. Owing to this fact, the process of tunneling of light in coupled strongly anisotropic fibers would also resemble the one in coupled ideal fibers. The main difference between these two situations is that, in coupled anisotropic fibers, the light upon tunneling would simultaneously assume the corresponding polarization. For an array of such anisotropic fibers, the overall picture would not change—the supermode would be given by the same combination of individual fiber modes, as in the case of an ideal fiber array, save for the difference that each constituent local fiber mode should have the polarization marker.

These arguments could be rendered in a mathematical form. The scalar waveguide equation for the system in question can be set as

$$\left(\nabla_t^2 + k^2\hat{n}^2\right)\mathbf{e}_t = \tilde{\beta}^2\mathbf{e}_t, \tag{2}$$

where $\nabla_t = (\partial/\partial x, \partial/\partial y)$, $\mathbf{e}_t(x,y)$ is the transverse part of the electric field (we use the notations adopted in Ref. [27]), $\tilde{\beta}$ is the scalar propagation constant, and the global Cartesian coordinates (x,y,z) are implied. The refractive index can be represented in the form

$$\hat{n}^2 = n_{cl}^2 + \sum_{j=0}^{N-1} f_j(x,y)\left[\left(n_{co}^2 - n_{cl}^2\right) + n_{co}\Delta n\, D\left(\gamma_j^p\right)\right], \tag{3}$$

where f_j is the cutoff factor, which is zero outside the core of the jth fiber and unity within the core, $D(\gamma_j^p) \equiv \left(\begin{smallmatrix} \cos 2\gamma_j^p & -\sin 2\gamma_j^p \\ -\sin 2\gamma_j^p & -\cos 2\gamma_j^p \end{smallmatrix}\right)$. The matrix D in Eq. (3) appears due to transformations of the refractive index tensors $\hat{n}_{t,j}^2$, which are diagonal in the frames connected with anisotropy axes, to the global Cartesian frame $\hat{n}_{t,j}^2 = \mathrm{diag}(n_e^2, n_o^2) \to R(\alpha)\hat{n}_{t,j}^2 R^T(\alpha)$, where $R(\alpha) = \left(\begin{smallmatrix} \cos\alpha & \sin\alpha \\ -\sin\alpha & \cos\alpha \end{smallmatrix}\right)$ is the operator of rotation through an angle α and T stands for transposition. In the case of a paraxial propagation of the field and a weak coupling that ensures power orthogonality, for finding the supermodes, one can use a simplified method based on the formalism of the perturbation theory modification for coupled fibers [28]. According to this formalism, one should build the matrix of the total operator on the left of (2) over the basis of any complete set of eigenvectors of such part of that operator for which the solution of the eigenvector problem is known for infinitely spaced fibers. Then, the modes of the system can be found by solving the eigenvector problem for the obtained matrix. Such a basis-generating operator can be chosen by setting $\Delta n = 0$in Eq. (3). One can take the basic solutions in the form of fundamental modes polarized along x and y axes of the global Cartesian frame and localized on the jth fiber,

$$|1,j\rangle = |x,j\rangle\,, \qquad |2,j\rangle = |y,j\rangle\,, \tag{4}$$

where the first index in the right-hand side ket vector specifies the direction of polarization, whereas, the second one describes the localization of the field. For example, the explicit expression for the first basic vector is as follows: $|1,j\rangle \equiv \left(\begin{smallmatrix}1\\0\end{smallmatrix}\right)F_0(r_j)$, where r_j is the local axial-polar coordinate in the frame associated with the jth fiber (see Fig. 1), F_0 is the radial function of the step-index fiber's fundamental mode, and the basis of linear polarizations $|e\rangle = \mathrm{col}(e_x, e_y)$ is implied.

In the nearest-neighbor approximation, the perturbation matrix reads as

$$M = \begin{pmatrix} \delta D\left(\gamma_0^p\right) & a\hat{1} & 0 & \cdots & 0 & a\hat{1} \\ a\hat{1} & \delta D\left(\gamma_1^p\right) & a\hat{1} & 0 & \cdots & 0 \\ 0 & a\hat{1} & \delta D\left(\gamma_2^p\right) & a\hat{1} & 0 & \cdots \\ \cdots & 0 & \cdots & \cdots & a\hat{1} & 0 \\ 0 & \cdots & 0 & a\hat{1} & \delta D\left(\gamma_{N-2j}^p\right) & a\hat{1} \\ a\hat{1} & 0 & \cdots & 0 & a\hat{1} & \delta D\left(\gamma_{N-1}^p\right) \end{pmatrix}, \tag{5}$$

where $\hat{1}$ is a rank-2 unity matrix. It is convenient here to pass to the basis connected with local anisotropy axes. It is effectively achieved by making the transform,

$$M \to M' = A(-\gamma)MA(\gamma), \tag{6}$$

where the transformation matrix is block diagonal $A(\gamma) = \mathrm{diag}[R(\gamma_0^p), R(\gamma_1^p), \ldots, R(\gamma_{N-1}^p)]$. Under the transform Eq. (6), the matrix M gets converted into the following rank-$2N$ block matrix:

$$M' = \begin{pmatrix} \delta\sigma_z & aR(\varphi_p) & 0 & \cdots & 0 & aR(\varphi_p) \\ aR(-\varphi_p) & \delta\sigma_z & aR(\varphi_p) & 0 & \cdots & 0 \\ 0 & aR(-\varphi_p) & \delta\sigma_z & aR(\varphi_p) & 0 & \cdots \\ \cdots & 0 & \cdots & \cdots & aR(\varphi_p) & 0 \\ 0 & \cdots & 0 & aR(-\varphi_p) & \delta\sigma_z & aR(\varphi_p) \\ aR(-\varphi_p) & 0 & \cdots & 0 & aR(-\varphi_p) & \delta\sigma_z \end{pmatrix}, \tag{7}$$

where σ_z is the Pauli matrix. In this rank-$2N$ matrix, odd columns and lines correspond to locally x-polarized vectors located in individual sites. At $\delta \gg a$, the eigenvectors of this matrix can be found by perturbation theory with degeneracy. Indeed, at $a = 0$, there are two N-fold degenerate eigenvalues $\pm\delta$: Locally x-polarized zero-approximation eigenvectors $|1,j\rangle$ belong to the positive eigenvalue, whereas, locally y-polarized eigenvectors $|2,j\rangle$ belong to the negative eigenvalue.

Building the corresponding perturbation matrices on the basis of matrix M' (in this simple case, it can be accomplished by canceling the corresponding lines and columns), one can establish that the structure of normal modes in the subspaces of both locally x- and y-polarized zero-approximation eigenvectors is determined by the same rank-N matrix P,

$$P = a\cos\varphi_p \begin{pmatrix} 0 & 1 & 0 & \cdots & 0 & 1 \\ 1 & 0 & 1 & 0 & \cdots & 0 \\ 0 & 1 & 0 & \cdots & 0 & \cdots \\ \cdots & 0 & \cdots & \cdots & 1 & 0 \\ 0 & \cdots & 0 & 1 & 0 & 1 \\ 1 & 0 & \cdots & 0 & 1 & 0 \end{pmatrix}. \quad (8)$$

This matrix is also known to determine the structure of supermodes in circular arrays of ideal fibers [22]. Using the well-known results, one can obtain the expressions for supermodes $\mathbf{X}_m$ and $\mathbf{Y}_m$ of the array of anisotropic fibers,

$$\mathbf{X}_m = \frac{1}{\sqrt{N}}\sum_{j=0}^{N-1}\exp(i\varphi_m j)Q_j\mathbf{i}'_j,$$
$$\mathbf{Y}_m = \frac{1}{\sqrt{N}}\sum_{j=0}^{N-1}\exp(i\varphi_m j)Q_j\mathbf{j}'_j, \quad (9)$$

where $m = 0,1,\ldots,N-1$, $\mathbf{i}'_j$ and $\mathbf{j}'_j$ are unit vectors directed along the x' and y' axes of local coordinate frames associated with the jth fiber and Q_j is the fundamental mode's wave function located on the jth site. The spectra, which correspond to the modes in Eq. (9), are as follows:

$$\beta_m^x = \tilde{\beta} + \frac{\delta}{2\tilde{\beta}} + \frac{a\cos\varphi_p}{2\tilde{\beta}}\cos\varphi_m,$$
$$\beta_m^y = \tilde{\beta} - \frac{\delta}{2\tilde{\beta}} + \frac{a\cos\varphi_p}{2\tilde{\beta}}\cos\varphi_m. \quad (10)$$

Since, for weakly guiding fibers, one has $\tilde{\beta} \approx kn_{co}$, the second terms on the right could also be represented as $\pm k\,\Delta n/2$. In this way, the spectrum of the array of anisotropic fibers is given by two sets of branches, which are strongly spaced due to anisotropy and consist of N branches (each set) with much less separation caused by interfiber coupling. The coupling constant a, in this case, is modulated by the factor $\cos\varphi_p$, which depends on the angle between the anisotropy axes of the neighboring fibers.

III. VORTEX STRUCTURE OF SUPERMODES AND THEIR ANGULAR MOMENTUM

Although the main importance of Eqs. (9) and (10) is in their ability to make predicting the amplitudes at the sites in an arbitrary cross section of the array possible, recent papers have evoked a large amount of interest in field behavior outside the vertices of the fiber array. One of their main questions has become the question about the kind of field which is formed outside the vertices [22,29]. In essence, this question is also characteristic to the studies of beam arrays [30]. Research has established that, for the circular array of ideal fibers in the center of the array, the DV is formed, whose topological charge is determined by the index m of the supermode. In this connection, it is interesting to study whether this situation has any analogies with the array of anisotropic fibers.

A. Discrete vortices and supermodes

Following the ideas of Refs. [22,30], let us consider the structure of the field of the modes in Eq. (9) in the transverse plane outside the vertices. The scalar amplitude of an individual jth fiber can be represented in the Gaussian approximation as [27]

$$Q_j = E\exp\left(-\frac{r_j^2}{2\rho^2}\right), \quad (11)$$

where E is some constant, ρ is the effective radius of the fundamental mode defined for step-index fibers as $\rho = \frac{\rho_0}{\sqrt{2\ln V}}$, ρ_0 being the core's radius and V being the waveguide parameter. Here, r_j is measured from the center of the jth core (see Fig. 1). Since $r_j^2 = r^2 + r_0^2 - 2rr_0\cos(\varphi - \varphi_j)$, where r_0 is the radius of the array and (r,φ,z) are the global axial polar coordinates, the projections $\Psi_{x,y}$ of the total field of the supermode $\mathbf{X}_m$ can be written as

$$\Psi_x^{(m,p)} = E\Gamma\sum_{j=0}^{N-1}\exp[z\cos(\varphi-\varphi_j) + im\varphi_j]\cos\gamma_j^p,$$
$$\Psi_y^{(m,p)} = E\Gamma\sum_{j=0}^{N-1}\exp[z\cos(\varphi-\varphi_j) + im\varphi_j]\sin\gamma_j^p, \quad (12)$$

where $\Gamma = E\exp(-\frac{r^2+r_0^2}{2\rho^2})$, $z = \frac{rr_0}{\rho^2}$. Analogous projections $\Phi_{x,y}$ for the supermode $\mathbf{Y}_m$ read as

$$\Phi_x^{(m)} = -E\Gamma\sum_{j=0}^{N-1}\exp[z\cos(\varphi-\varphi_j) + im\varphi_j]\sin\gamma_j^p,$$
$$\Phi_y^{(m)} = E\Gamma\sum_{j-0}^{N-1}\exp[z\cos(\varphi-\varphi_j) + im\varphi_j]\cos\gamma_j^p. \quad (13)$$

To determine the asymptotical behavior of the fields in Eqs. (12) and (13) at the origin $r = 0$, one should use a well-known decomposition [22],

$$\exp(z\cos\alpha) = \sum_{n=-\infty}^{\infty} I_n(z)\exp(in\alpha), \quad (14)$$

where I_k is the Bessel function. With the help of a special summation rule,

$$\sum_{j=0}^{N-1}\exp(il\varphi_j) = N\delta_{l,mN}, \quad (15)$$

where $\delta_{l,m}$ is the Kronecker δ and $m = 0, \pm 1, \pm 2, \ldots$, which has been first suggested in Ref. [26] and is a generalization of the standard widespread expression obtained from Eq. (15) at $m = 0$, one can get, for the field's asymptotics,

$$\Psi_x^{(m,p)} = \frac{1}{2}N\Gamma\sum_{l=-\infty}^{\infty}\{I_{lN+m+p}(z)\exp[i(lN+m+p)\varphi]$$
$$+I_{lN+m-p}(z)\exp[i(lN+m-p)\varphi]\},$$

$$\Psi_y^{(m,p)} = -\frac{i}{2}N\Gamma\sum_{l=-\infty}^{\infty}\{I_{lN+m+p}(z)\exp[i(lN+m+p)\varphi] -I_{lN+m-p}(z)\exp[i(lN+m-p)\varphi]\}, \quad (16)$$

Analogous expressions can be obtained for the y'-polarized modes in Eq. (13).

In the same manner as was performed in Ref. [22], one can establish the topological charge $\Im$, which the supermode bears in each of the linearly polarized components. It is determined by the lowest by modulus order and the largest at $r \sim 0$ of Bessel functions, which enter the sums in Eq. (16) (we allow for $I_\nu = I_{-\nu}$),

$$|\Im| = \min_l\{|lN+m+p| \bmod N, |lN+m-p| \bmod N\}. \quad (17)$$

This relation demonstrates that the topological charge in the field's components also is determined by the index p of the director's rotation. In this way, one can affect $\Im$ by changing the pattern of anisotropy axes' orientation. This circumstance proves crucial for the ability to control the topological charge through the polarization distribution. One should note that the charges in both x- and y-polarized components appear to be the same. More elegant is the expression for $\Im$ in circularly polarized components. For $\mathbf{X}_m$ supermodes, one obtains the following expression for the field vector:

$$\Psi^{(m,p)} = \frac{1}{2}N\Gamma\sum_{l=-\infty}^{\infty}\{\mathbf{c}_+I_{lN+m+p}(z)\exp[i(lN+m+p)\varphi]\} +\mathbf{c}_-I_{lN+m-p}(z)\exp[i(lN+m-p)\varphi], \quad (18)$$

where $\mathbf{c}_\pm = \mathbf{i} \mp i\mathbf{j}$ are the vectors of a circular basis. Analogously, for $\mathbf{Y}_m$ supermodes, one has

$$\Phi^{(m,p)} = \frac{i}{2}N\Gamma\sum_{l=-\infty}^{\infty}\{\mathbf{c}_+I_{lN+m+p}(z)\exp[i(lN+m+p)\varphi] -\mathbf{c}_-I_{lN+m-p}(z)\exp[i(lN+m-p)]\varphi\}. \quad (19)$$

The charges of these fields are found in a less ambiguous fashion,

$$|\Im| = \min_l\{|lN+m\pm p| \bmod N\}, \quad (20)$$

where the upper sign should be taken for right-hand polarization. Comparison with the corresponding results of Ref. [22] shows that, here, the charge is determined not just by the modal index m, but rather by its combination with the index p of polarization rotation $m \pm p$.

As is known, these fields in the modes' components represent phase distribution characteristic to DVs, which are currently being widely studied [31]. Since, for these fields, the phase distribution over any circular contour with the center on the array's symmetry axis has a specific steplike form, this enables us to identify the fields in orthogonal components of the mth supermode with the DVs of charge $\Im$ [22]. In a particular case $N = 2(m \pm p)$, no DV is formed in the field components. Instead, multifold edge dislocations are formed. In the same way, due to the topological charge "stroboscopic" effect, it is impossible to create a supermode with the topological charge of more than $N/2$ in a component. Comparing Eqs. (17) and (20), one can state that, generally, linearly and circularly polarized components of the supermode's field nestle OVs of different topological charges. This fact is well known in singular optics and relates to the ability of a circular polarizer to render topological charge to vectorial fields. Basically, this should be considered in the context of a quantum-mechanical concept of changing the system's state upon measurement procedure and underlies the recently reported generation of OVs through a fiber's output [32]. It should be emphasized that studying the structure of polarization singularities in the supermodes' fields lies far beyond the scope of this paper, although it could be the subject of a special study.

B. Angular momentum of supermodes

Although there is no rigid connection between AM and the presence of OVs in the field, AM is an important characteristic of the light field and its flows of energy [33]. Following Berry [34], we calculate the ratio of the time-averaged z component of AM linear density M_z (AM density integrated over a cross section) to the time-averaged linear energy density W as

$$\frac{M_z}{W} = \frac{1}{\omega}\frac{\langle\psi|\,l_z+\sigma_z\,|\psi\rangle}{\langle\psi|\,\psi\rangle}, \quad (21)$$

where $l_z = -i\partial/\partial\varphi$, ω is the frequency, and the representation in the basis of circular polarizations is adopted: $|\psi\rangle = \mathrm{col}(\psi_+,\psi_-)$, $\psi_\pm = \frac{1}{\sqrt{2}}(e_x \mp ie_y)$. Here, the Dirac product is defined as

$$\langle a \mid b\rangle = \int\int_\Sigma (a_1^*,a_2^*)\begin{pmatrix} b_1 \\ b_2 \end{pmatrix} dS, \quad (22)$$

where Σ is the total transverse cross section.

The vectorial case for circular arrays can be easily reduced to the well-studied scalar one. Indeed, expanding the nominator and denominator in Eq. (21), one can obtain

$$\begin{aligned}\langle\psi|\,l_z+\sigma_z\,|\psi\rangle &= (\psi_+,l_z\psi_+)+(\psi_-,l_z\psi_-)+(\psi_+,\psi_+)-(\psi_-,\psi_-)\\ &\equiv L_z+S_z,\\ \langle\psi|\,\psi\rangle &= (\psi_+,\psi_+)+(\psi_-,\psi_-),\end{aligned} \quad (23)$$

where $(\ldots,\ldots)$ stands for a scalar product of functions. The first two terms in relation to the AM in Eq. (23) represent the OAM L_z, whereas, the last terms should be identified with the spin AM (SAM). Using the corresponding result of Ref. [22], for these constituents, one can obtain the following expressions for the mth supermode:

$$L_z = NE^2\pi r_0^2\sum_{n=0}^{N-1}\sin\,\varphi_n\,\sin(m\varphi_n)\cos(p\varphi_n) \times \exp\left(-\frac{r_0^2}{\rho^2}\sin^2\frac{\varphi_n}{2}\right), \quad (24)$$

$$S_z = 2NE^2\pi\rho^2\sum_{n=0}^{N-1}\sin(m\varphi_n)\sin(p\varphi_n)\exp\left(-\frac{r_0^2}{\rho^2}\sin^2\frac{\varphi_n}{2}\right), \quad (25)$$

$$w = 2NE^2\pi\rho^2\sum_{n=0}^{N-1}\cos(m\varphi_n)\cos(p\varphi_n)\exp\left(-\frac{r_0^2}{\rho^2}\sin^2\frac{\varphi_n}{2}\right). \quad (26)$$

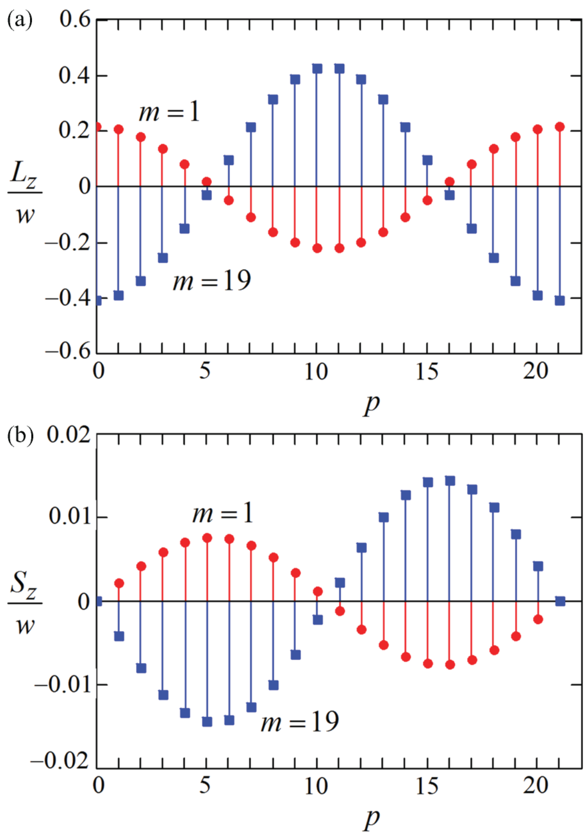

FIG. 2. (Color online) (a) Specific orbital angular momentum and (b) specific spin angular momentum of certain supermodes vs the array's index p. Array's parameters: $N = 21$, $r_0/\rho = 14$. The number m of the supermode is indicated near the corresponding set of points.

Note that, since these quantities have the same dimension and are just proportional to exact angular momenta and energy of the system, they should be used only in the context of Eq. (21). Figure 2 represents the dependence of specific orbital [Fig. 2(a)] and spin [Fig. 2(b)] angular momenta of certain supermodes on the array's index p. As is seen, OAM periodically depends on p, which reflects the influence of the stroboscopic topological charge rule, given in Eq. (20). The SAM turns out to be almost equal to zero, which corresponds to almost linear polarization of the field of the supermodes.

IV. FIBER-ARRAY ANALOG OF *Q* PLATES

Although establishing the vortex composition of supermodes is important, finding out the mode structure is usually an intermediate result. More practically relevant are the transformation properties of the system since it often proves difficult to generate the field distribution characteristic to a pure mode at the input of the array. In a general case, one encounters the problem of establishing the evolution of the state excited at the input end of the array. In arrays of ideal fibers, which can be described by scalar functions, it is usually assumed that the energy is localized at the sites of the lattice and its distribution is determined by squared moduli of the field amplitudes at the fibers so that such distribution is characterized with the set of squared amplitudes. In the vectorial case, such sets should be multiplied (doubled in our situation) to present boundary conditions for each polarization. Let the amplitudes at $z = 0$ be described by two N-dimensional vectors $\mathbf{I} = \mathrm{col}(I_0 \cdots I_{N-1})$ and $\mathbf{J} = \mathrm{col}(J_0 \cdots J_{N-1})$, where I_i and J_i stand for the amplitudes of x- and y-polarized fields at the ith fiber, correspondingly. Note that we define the initial state Ξ in the global Cartesian basis so that

$$\Xi(z = 0) = \sum_{n=0}^{N-1} (I_n Q_n \mathbf{i} + J_n Q_n \mathbf{j}). \tag{27}$$

Decomposing this field over the array's modes in Eq. (9) $\Xi(z = 0) \equiv \sum_{n=0}^{N-1} (c_n \mathbf{X}_n + d_n \mathbf{Y}_n)$, one can obtain the expressions for the desired expansion coefficients c_n, d_n,

$$c_n = \frac{1}{\sqrt{N}} \sum_{j=0}^{N-1} [I_j \cos(\varphi_p j) + J_j \sin(\varphi_p j)] \exp(-i\varphi_n j),$$
$$d_n = \frac{1}{\sqrt{N}} \sum_{j=0}^{N-1} [-I_j \sin(\varphi_p j) + J_j \cos(\varphi_p j)] \exp(-i\varphi_n j). \tag{28}$$

After a little algebra, one can obtain the expressions for vectorial amplitudes at the nth fiber in a cross section with coordinate z,

$$\begin{aligned} {}^{p}_{n,x} = \frac{1}{N} \sum_{m,l=0}^{N-1} \bigg\{ & [I_l \cos(\varphi_p l) + J_l \sin(\varphi_p l)] \cos(\varphi_p n) \exp\left(\frac{i}{2} k\, \Delta n\, z\right) - [-I_l \sin(\varphi_p l) + J_l \cos(\varphi_p l)] \sin(\varphi_p n) \\ & \times \exp\left(-\frac{i}{2} k\, \Delta n\, z\right) \bigg\} \exp[i\varphi_m (n - l)] \exp\left(\frac{iaz}{kn_{co}} \cos\varphi_p \cos\varphi_m\right), \\ A^{p}_{n,y} = \frac{1}{N} \sum_{m,l=0}^{N-1} \bigg\{ & [I_l \cos(\varphi_p l) + J_l \sin(\varphi_p l)] \sin(\varphi_p n) \exp\left(\frac{i}{2} k\, \Delta n\, z\right) + [-I_l \sin(\varphi_p l) + J_l \cos(\varphi_p l)] \cos(\varphi_p n) \\ & \times \exp\left(-\frac{i}{2} k\, \Delta n\, z\right) \bigg\} \exp[i\varphi_m (n - l)] \exp\left(\frac{iaz}{kn_{co}} \cos\varphi_p \cos\varphi_m\right). \end{aligned} \tag{29}$$

These expressions answer the question of evolution of the arbitrary state excited at the input end of the circular array of strongly anisotropic fibers.

To make parallels with the known properties of the q plates, one should note that one of the main features of q plates is their ability to transform a circularly polarized Gaussian beam into an OV. Although, actually, to the best of our knowledge, no rigorous theoretical treatment of this process has been presented in the literature, which would have shown the origin of a zero-amplitude vortex line out of Gaussian profile, the reliability of those devices has been convincingly proven in a vast body of experimental research [18]. It is, therefore, natural to study how the p array transforms the set of fundamental circularly polarized modes, which it is excited with. In this case, the boundary condition is as follows:

$$I_l = I, \quad J_l = i\sigma I, \tag{30}$$

where $\sigma = \pm 1$ allows for the type of circular polarization. Using Eqs. (29), one can readily obtain the following expressions for complex amplitudes in orthogonal polarizations. It is convenient to represent the field in the circular basis,

$$\begin{aligned} A^p_{n,+} &= I\left\{\exp\left(\frac{i}{2}k\,\Delta n\,z\right) + \sigma\,\exp\left(-\frac{i}{2}k\,\Delta n\,z\right)\right\} \\ &\quad\times \exp[i\varphi_p n(\sigma-1)]\exp\left(\frac{iaz}{kn_{co}}\cos^2\varphi_p\right), \\ A^p_{n,-} &= I\left\{\exp\left(\frac{i}{2}k\,\Delta n\,z\right) - \sigma\,\exp\left(-\frac{i}{2}k\,\Delta n\,z\right)\right\} \\ &\quad\times \exp[i\varphi_p n(\sigma+1)]\exp\left(\frac{iaz}{kn_{co}}\cos^2\varphi_p\right). \end{aligned} \tag{31}$$

As is evident from these expressions, there are two scales of spatial evolution of the state in this case. The small one is determined by birefringence in individual fibers. The large scale is governed by the exchange constant a and is connected with the energy exchange between the fibers, which is responsible for smooth variations in amplitudes. It is remarkable that these physical processes completely factorize and do not affect each other. Moreover, the main part belongs to the birefringence effect since it governs amplitudes of the components.

From Eqs. (31), the transformation properties of p arrays are easily derived. Indeed, let us take, for definiteness, $\sigma = 1$. Then, the components assume the form

$$\begin{aligned} A^p_{n,+} &\propto \cos\left(\tfrac{1}{2}k\,\Delta n\,z\right), \\ A^p_{n,-} &\propto \sin\left(\tfrac{1}{2}k\,\Delta n\,z\right)\exp\left(2i\varphi_p n\right). \end{aligned} \tag{32}$$

To avoid misunderstanding, it should be emphasized that, in Eqs. (31), only the exponentials with the factor $\varphi_p n$ describe the modulation of phase over the array, which is responsible for the appearance of the DV. The exponentials of $\cos^2\varphi_p$ stand for phase modulation over z and contribute only to the appearance of the total phase, which does not depend on the number n of the site and, therefore, can be neglected. As is evident from these relations, in certain cross sections determined by the equation $\cos(\frac{1}{2}k\,\Delta n\,z) = 0$, the field in each site would be circularly polarized and the phase increment between the neighboring fibers would equal $2\varphi_p$. In this way, the p array would generate a DV with the topological charge determined by the array's index p in those cross sections,

$$\Im = \begin{cases} 2p, & \text{at} \quad N > 4p, \\ 2p - N, & \text{at} \quad N < 4p. \end{cases} \tag{33}$$

In the particular case $N = 4p$, which can be achieved only for arrays with the even number of fibers, the field would represent a $2p$-fold edge dislocation [22]. Note that, due to topological charge stroboscopic effect, it is also impossible to generate a supermode with the topological charge of more than $N/2$ in p arrays. As follows from Eq. (31), for $\sigma = -1$ in certain cross sections determined by the same condition, the p array would generate the DV of the opposite value. In this way, p arrays enable polarization control over phase singularities. This is the main result of the present paper.

Comparing these results with the known facts for the q plates, one can reveal complete analogy in transformation properties of these two optical systems. Indeed, Eq. (30) is equivalent to Eq. (10), obtained by Marucci in Ref. [18]: One of the components at arbitrary z always nestles the OV, whereas, the other component carries a regular optical field. However, despite this obvious similarity, there are essential differences between these systems. First, the charge of the outcoming vortex in a p array is not simply proportional to the number p of the anisotropy director's full rotations as it takes place for q plates. The charge given by Eq. (33) cannot exceed $N/2$ and decreases for larger values of p due to the stroboscopic effect, whereas, for q plates, there is no such parameter as N and $\Im = 2p$. It should be noted that this difference is preserved even in the limit $N \to \infty$ (at the increasing radius of the ring, this limit could be made quite physical) so that continuous distribution is never achieved at any step of the succession of approximations. In our opinion, this situation could be described using the notion of a singular limit [34]. Second, generated in p arrays, OVs rather belong to the class of discrete vortices than to conventional OVs generated in q plates so that such arrays can be considered as generators of DVs. The third comment that should be made concerns the semblance of Eq. (31) and Eq. (10) of Marucci [18]. It is remarkable that Eq. (31), obtained through a rigorous formalism and valid for any z, coincides in its main features with an approximate Eq. (10) of Ref. [18], suitable for description of relatively thin q plates. This proves the reliability of the simple model approach based on the Jones formalism suggested in that insightful paper. As for bulk plates with engineered distribution of anisotropy axes, the solution of this problem has also been reported [35] and has been experimentally verified [36]. One can also mention recent examples of solving the analogous problems [37]. Finally, it should be emphasized that the results obtained are valid only for integer values of the array's parameter p. At half-integer p, a sort of discontinuity in the anisotropy director's behavior takes place, and a substantial revision of the theory might be in order. Recently obtained experimental results, however, demonstrate that, even in this case, the p arrays maintain semblance with the q plates and are able to generate vortex beams from a Gaussian-like input [38].

V. CONCLUSION

In this paper, we have studied propagation of light in a p array, that is, a circular array of strongly anisotropic fibers in which the orientation of the anisotropy director linearly depends on the angular position of the fiber in the array and the director makes an integer number of full rotations p while tracing along the contour of the array. We have obtained the spectrum and the structure of supermodes for such a system and have shown that they consist of two discrete optical vortices nestled in the opposite circular polarizations. We have found the expressions for topological charges of such vortices. We have also studied the angular momentum carried by these supermodes. We have obtained the expression for the evolution of an arbitrary excitation created at the array's input upon its discrete diffraction over the array. As an application of such expressions, we have examined the propagation of the set of circularly polarized fundamental modes excited at the input end with equal weights and phases. We have demonstrated that, in certain cross sections, the p array generates a discrete circularly polarized optical vortex, whose topological charge is determined by the array's index p. In this way, we have shown that the p arrays enable polarization control over phase singularities and, in this way, are discrete analogs of the q plates.

ACKNOWLEDGMENTS

The author acknowledges useful discussions with M. A. Yavorsky and is grateful for his technical assistance.

[1] J. F. Nye and M. V. Berry, Proc. R. Soc. London, Ser. A **336**, 165 (1974).

[2] *Optical Vortices*, Horizons of World Physics, Vol. 228, edited by M. Vasnetsov and K. Staliunas (Nova Science Publishers, New York, 1999); G. Indebetouw, J. Mod. Opt. **40**, 73 (1993); A. V. Volyar and T. A. Fadeeva, Opt. Spectrosc. **85**, 272 (1998).

[3] M. S. Soskin and M. V. Vasnetsov, Prog. Opt. **42**, 219 (2001).

[4] M. V. Berry, in *Singularities in Waves*, edited by R. Balian, M. Kléman, and J.-P. Poirier, Les Houches Lecture Series Session XXXV (North-Holland, Amsterdam, 1981), pp. 453–543; J. F. Nye, *Natural Focusing and Fine Structure of Light: Caustics and Wave Dislocations* (Institute of Physics Publishing, Bristol, 1999).

[5] I. Freund, Opt. Commun. **201**, 251 (2002); G. M. Philip, V. Kumar, G. Milione, and N. K. Viswanathan, Opt. Lett. **37**, 2667 (2012); I. Freund, *ibid.* **37**, 2223 (2012); V. A. Makarov, I. A. Perezhogin, and N. N. Portavkin, J. Opt. **14**, 055202 (2012); M. R. Dennis, Opt. Lett. **36**, 3765 (2011); Y. V. Jayasurya, V. V. G. K. Inavalli, and N. K. Viswanathan, Appl. Opt. **50**, E131 (2011).

[6] S. B. Raghunathan, H. F. Schouten, and T. D. Visser, Opt. Lett. **37**, 4179 (2012); C. Rosenbury, Y. Gu, and G. Gbur, J. Opt. Soc. Am. A **29**, 410 (2012).

[7] M. R. Dennis, Y. S. Kivshar, M. S. Soskin, and G. A. Swartzlander, Jr., J. Opt. A, Pure Appl. Opt. **11**, 090201 (2009).

[8] M. V. Berry, J. Opt. A, Pure Appl. Opt. **6**, S178 (2004).

[9] V. S. Liberman and B. Y. Zel'dovich, Phys. Rev. A **45**, 5199 (1992); A. V. Dooghin, N. D. Kundikova, V. S. Liberman, and B. Y. Zel'dovich, *ibid.* **45**, 8204 (1992); K. Y. Bliokh and Y. P. Bliokh, Phys. Lett. A **333**, 181 (2004); C. N. Alexeyev, Y. A. Fridman, and A. N. Alexeyev, Ukr. J. Phys. **44**, 74 (1999); A. V. Volyar, V. Z. Zhilaitis, and V. G. Shvedov, Opt. Spectrosc. **86**, 593 (1999); K. N. Alekseev, A. V. Volyar, and T. A. Fadeeva, *ibid.* **93**, 588 (2002); C. C. Leary, M. J. Raymer, and S. J. van Enk, Phys. Rev. A **80**, 061804(R) (2009).

[10] S. Mosca, B. Canuel, E. Karimi, B. Piccirillo, L. Marrucci, R. De Rosa, E. Genin, L. Milano, and E. Santamato, Phys. Rev. A **82**, 043806 (2010); J. M. Amjad, H. R. Khalesifard, S. Slussarenko, E. Karim, L. Marrucci, and E. Santamato, Appl. Phys. Lett. **99**, 011113 (2011); O. G. Rodriguez-Herrera, D. Lara, K. Y. Bliokh, E. A. Ostrovskaya, and C. Dainty, Phys. Rev. Lett. **104**, 253601 (2010); X. Lu and L. Chen, Opt. Express **20**, 11753 (2012); I. Skab, Y. Vasylkiv, I. Smaga, and R. Vlokh, Phys. Rev. A **84**, 043815 (2011); T. Fadeyeva, A. Rubass, Y. Egorov, A. Volyar, and G. Swartzlander, Jr., J. Opt. Soc. Am. A **25**, 1634 (2008); T. A. Fadeyeva, V. G. Shvedov, Y. V. Izdebskaya, A. V. Volyar, E. Brasselet, D. N. Neshev, A. S. Desyatnikov, and Y. S. Kivshar, Opt. Express **18**, 10848 (2010); V. G. Shvedov, Y. V. Izdebskaya, A. N. Alekseev, and A. V. Volyar, Tech. Phys. Lett. **28**, 256 (2002); Y. V. Izdebskaya, V. G. Shvedov, and A. V. Volyar, Opt. Lett. **30**, 2530 (2005).

[11] M. El Ketara and E. Brasselet, Opt. Lett. **37**, 602 (2012); E. Brasselet, Phys. Rev. A **82**, 063836 (2010); E. Brasselet and C. Loussert, Opt. Lett. **36**, 719 (2011).

[12] K. Y. Bliokh, M. A. Alonso, E. A. Ostrovskaya, and A. Aiello, Phys. Rev. A **82**, 063825 (2010).

[13] O. Hosten and P. Kwiat, Science **319**, 787 (2008).

[14] M. Kang, J. Chen, B. Gu, Y. Li, L. T. Vuong, and H.-T. Wang, Phys. Rev. A **85**, 035801 (2012); I. Skab and R. Vlokh, Appl. Opt. **51**, C22 (2012).

[15] L. Marrucci, C. Manzo, and D. Paparo, Phys. Rev. Lett. **96**, 163905 (2006); Appl. Phys. Lett. **88**, 221102 (2006); F. Cardano, E. Karimi, S. Slussarenko, L. Marrucci, C. de Lisio, and E. Santamato, Appl. Opt. **51**, C1 (2012); E. Karimi, S. Slussarenko, B. Piccirillo, L. Marrucci, and E. Santamato, Phys. Rev. A **81**, 053813 (2010).

[16] R. Bhandari, Phys. Rep. **281**, 1 (1997).

[17] G. Biener, A. Niv, V. Kleiner, and E. Hasman, Opt. Lett. **27**, 1875 (2002); Z. Bomzon, G. Biener, V. Kleiner, and E. Hasman, *ibid.* **27**, 1141 (2002).

[18] L. Marrucci, E. Karimi, S. Slussarenko, B. Piccirillo, E. Santamato, E. Nagali, and F. Sciarrino, J. Opt. **13**, 064001 (2011); L. Marrucci, Mol. Cryst. Liq. Cryst. **488**, 148 (2008).

[19] H. Kawauchi, Y. Kozawa, S. Sato, T. Sato, and S. Kawakami, Opt. Lett. **33**, 399 (2008); G. Machavariani, Y. Lumer, I. Moshe, A. Meir, and S. Jackel, *ibid.* **32**, 1468 (2007).

[20] A. A. Sukhorukov, S. V. Dmitriev, S. V. Suchkov, and Y. S. Kivshar, Opt. Lett. **37**, 2148 (2012); D. Leykam and A. S. Desyatnikov, *ibid.* **36**, 4806 (2011); A. S. Desyatnikov, M. R. Dennis, and A. Ferrando, Phys. Rev. A **83**, 063822 (2011); H. Xu, J. Wu, K. Xu, Y. Dai, C. Xu, and J. Lin, J. Opt. **13**, 055405 (2011).

[21] Y. Yan, J. Wang, L. Zhang, J.-Y. Yang, I. M. Fazal, N. Ahmed, B. Shamee, A. E. Willner, K. Birnbaum, and S. Dolinar, Opt. Lett. **36**, 4269 (2011); Y. F. Yu, Y. H. Fu, X. M. Zhang *et al.*, Opt. Express **18**, 21651 (2010); R. S. Kurti, K. Halterman, R. K. Shori, and M. J. Wardlaw, *ibid.* **17**, 13982 (2009).

[22] C. N. Alexeyev, A. V. Volyar, and M. A. Yavorsky, Phys. Rev. A **80**, 063821 (2009).

[23] C. N. Alexeyev, A. V. Volyar, and M. A. Yavorsky, Phys. Rev. A **84**, 063845 (2011).

[24] E. Shafir, A. Hardy, and M. Tur, Opt. Lett. **12**, 1041 (1987); J. Lightwave Technol. **6**, 58 (1988).

[25] C. N. Alexeyev [Special issue in J. Opt. **15** (to be published)] (2013).

[26] *Selected Papers on Coupled-Mode Theory in Guided-Wave Optics*, edited by D. J. Hall, SPIE Milestone Series MS 84 (SPIE, Bellingham, Washington, 1993).

[27] A. W. Snyder and J. D. Love, *Optical Waveguide Theory* (Chapman and Hall, London/New York, 1985).

[28] C. N. Alexeyev, A. N. Alexeyev, N. A. Boklag, and M. A. Yavorsky, J.Opt. A, Pure Appl. Opt. **11**, 125404 (2009); C. N. Alexeyev, N. A. Boklag, and M. A. Yavorsky, J. Opt. **12**, 115704 (2010).

[29] R. S. Kurti, K. Halterman, R. K. Shori, and M. J. Wardlaw, Opt. Express **17**, 13982 (2009).

[30] Y. Izdebskaya, V. Shvedov, and A. Volyar, J. Opt. Soc. Am. A **25**, 171 (2008); Y. Izdebskaya, T. Fadeyeva, V. Shvedov, and A. Volyar, Opt. Lett. **31**, 2523 (2006).

[31] V. E. Lobanov, O. V. Borovkova, Y. V. Kartashov, B. A. Malomed, and L. Torner, Opt. Lett. **37**, 1799 (2012); Y. V. Kartashov, A. Ferrando, and M.-A. Garcia-March, *ibid.* **32**, 2155 (2009); M. Zacares, M. A. Garcia-March, J. Vijande, A. Ferrando, and E. Merino, Phys. Rev. A **80**, 043812 (2009); Y. V. Kartashov, B. A. Malomed, V. A. Vysloukh, and L. Torner, *ibid.* **80**, 053816 (2009); A. Ferrando, M. Zacares, and P. Andre, Opt. Express **13**, 1072 (2005).

[32] V. V. G. K. Inavalli and N. K. Viswanathan, Opt. Commun. **283**, 861 (2010).

[33] L. Allen, S. M. Barnett, and M. J. Padgett, *Optical Angular Momentum* (Institute of Physics Publishing, Bristol, 2003); A. Bekshaev, M. Soskin, and M. Vasnetsov, *Paraxial Light Beams with Angular Momentum* (Nova Science Publishers, New York, 2008); M. V. Berry, J. Opt. A, Pure Appl. Opt. **11**, 094001 (2009); A. Bekshaev, K. Y. Bliokh, and M. Soskin, J. Opt. **13**, 053001 (2011).

[34] M. V. Berry, Phys. Today **55**, 10 (2002).

[35] E. Karimi, B. Piccirillo, L. Marrucci, and E. Santamato, Opt. Lett. **34**, 1225 (2009).

[36] E. Karimi, B. Piccirillo, E. Nagali, L. Marrucci, and E. Santamato, Appl. Phys. Lett. **94**, 231124 (2009).

[37] T. A. Fadeyeva, C. N. Alexeyev, P. M. Anischenko, and A. V. Volyar, Appl. Opt. **51**, C224 (2012).

[38] G. Milione, H. I. Sztul, D. A. Nolan, J. Kim, M. Etienne, J. McCarthy, J. Wang, and R. R. Alfano, in Proc. SPIE: Complex Light and Optical Forces V **7950**, 79500K (2011).